ISBN: 978-3-95450-214-1 ISSN: 2673-5490 doi:10.18429/JACoW-IPAC2021-MOPAB098

LCLS MULTI-BUNCH IMPROVEMENT PLAN

A. Halavanau, A. Lutman, A. Krasnykh, D. Nguyen, S. Carbajo, C. Mayes, A. Marinelli, F. J. Decker
SLAC National Accelerator Laboratory, Stanford University, Menlo Park, CA, USA

Abstract

Current and future experiments at LCLS require XFEL pulse trains of variable time separation. The cavity based XFEL (CBXFEL) project requires multiple pulses separated by 220 ns, the X-ray Laser Oscillator (XLO) uses 15 ns spaced pulse trains and Matter under Extreme Conditions (MEC) experiments need a shortly spaced (less than 5 ns) pulse trains. In this proceeding, we discuss the LCLS multi-bunch improvement plan and report on its recently status and progress.

INTRODUCTION

The LCLS copper linac has been a backbone of the LCLS-I facility, as well as it is a significant part of the LCLS-II project. It accelerates electron beams, provided by a compact 135 MeV photoinjector. In the photoinjector, a strong UV pulse is impinging on a copper photocathode, generating up to 1 nC bunches per pulse. The linac consists of three (L1, L2, L3) S-band accelerating sections and one (L1X) 3rd harmonic cavity, as shown in Fig. 1, bringing the total electron beam energy to up 17 GeV. After initial acceleration in the photoinjector and linac section L1, the beam is compressed and collimated in the first bunch compressor (BC1). It is then transported through the linac section L2, compressed to the final fs-duration level in the second bunch compressor (BC2) and accelerated to the target beam energy in the linac section L3. The copper linac electron beam produces Angstrom-fs scale X-ray pulses in the HXR undulator, with the maximum photon energy of 20 keV.

Currently, the copper linac is mainly operated in a single pulse mode at a repetition rate of 120 Hz. It is, however, possible to operate it in the multi-bunch mode, with bunches separated by $n\tau$, where τ is 0.35 ns or the duration of one RF cycle and n is an integer. Multi-bunch mode has been previously tested in two- and four-bunch configuration with different spacings [1–4]. In this proceeding we are presenting a plan to improve the existing infrastructure and produce tunable bunch trains (1 - 220 ns) with 8 or possibly more bunches.

Multi-bunch operation of LCLS copper linac opens new experimental possibilities in FEL R&D, X-ray spectroscopy and MEC experiments. Currently at SLAC, a few science projects and experiments require pulse trains of 2/4/8 SASE pulses with various spacing: CBXFEL [5, 6] (2 bunches with ~ 220 ns spacing, with a stretch goal of 4 bunches), starting in 2022; XLO [7] (up to 8 bunches with 5-20 ns spacing), starting in 2021; MEC experiments (up to 8 bunches, 2-25 ns spacing), starting in 2021.

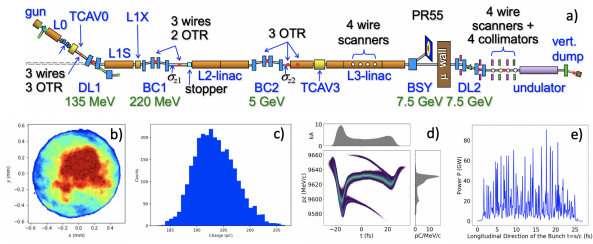

Figure 1: a) LCLS copper linac beamline schematics, b) Transverse profile of the UV laser at the photocathode location, c) Relative RMS bunch charge fluctuation after BC1, d) Longitudinal phase-space at the HXR undulator location and e) Resulting XFEL temporal pulse profile after the HXR undulator.

OVERVIEW OF MOST RECENT EXPERIMENTS

We have recently re-established multi-bunch capability at LCLS with the new HXR undulator. We have tested multiple separations of two bunches, generated independently by the two lasers. We were able to repeatedly reproduce similar SASE performance of the two bunches when the laser heater was used on both. Fast diodes can be used for registering the pulse train intensity as a function of time. For instance, Fig. 2 shows a trace of AXUV20HS1 photodiode illuminated by two XFEL pulses 30 ns apart.

We have also obtained 4 and 8 bunch trains using two lasers and a pulse stacker, with a very limited XFEL performance. These results will be reported elsewhere. In order to upgrade the UV pulse stacker performance we are considering a generation of IR pulse train, pulse energy replenishment in a Multipass Amplifier (MPA) and subsequent up-conversion to the UV.

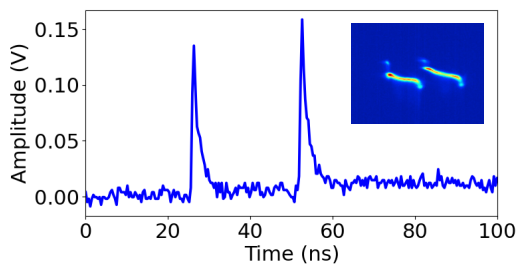

Figure 2: Fast diode waveform of the two laser heated pulses of about 30 ns apart. The inset contains the time-resolved longitudinal phase-space image.

ISBN: 978-3-95450-214-1 ISSN: 2673-5490 doi:10.18429/JACoW-IPAC2021-MOPAB098

IR PULSE TRAIN GENERATION

In the present photoinjector configuration, two Ti:Sapphire lasers generate ps-long IR pulses that are further frequency up-converted to UV range, and stacked in a train with two tunable split-and-delay lines. The two UV pulses can also bypass the split-and-delay line and directly overlap at the photocathode with an arbitrary time delay. Existing infrastructure contains two laser stations, Coherent 1 and 2, bringing the maximum possible number of pulses in the train to 8 in the current configuration. The physical size of the pulse stacker is a primary limitation to equispaced pulse trains. However two ns-spaced pairs of pulses can be separated by a few hundred ns, using two independent laser stations.

One of the main disadvantages of UV range pulse-stacking setup is the limited energy W_0 of the original UV pulse. The energy per pulse in the train is given by W_0/n, where n is the number of splittings. When $n > 4$, the UV laser intensity becomes too low for nominal photoinjector operation, and therefore for large pulse trains this setup is not practical.

An alternative approach is to generate pulse trains in the IR range; see Fig. 3. Since this pulse stacking method uses polarizers for splitting and combining laser pulses traversing different paths, the electric fields of the output laser pulses are polarized along two orthogonal directions. In order for both IR pulses to be amplified in the MPA, which is also polarization dependent as it uses polarizers for injecting the low-power input beam and ejecting the amplified beam, the polarization angles of both laser pulses have to be rotated by 45° before injection into the MPA. This is done with a HWP in front of the prism polarizer that injects one-half of the power in both laser pulses with s-polarization into the MPA. The other half of the IR power with p-polarization is transmitted and traverses another HWP that rotates its polarization by 90° before injection into the MPA. We select the optical path lengths of the two amplifier chain such that when the two sets of pulse pairs are combined, they form a train of laser pulses with variable separation and approximately equal amplitude. We can also correct for small variations in amplitude of the four IR pulses by adjusting the HWP angles and ramping the gain of the MPA. The spacing of the bunches will be limited, in principle, by the upper state lifetime of MPA's Ti:Saph of 3.2 µs.

The high-power IR pulses are converted to UV via two-stage third harmonic generation (THG). The first stage is a second harmonic generation (SHG) that converts 760-nm near-IR light to 380-nm deep blue light, followed by sum-frequency mixing of these wavelengths to produce the desired 253-nm UV light. We purposely choose to stack the pulses before the two stages of SHG so that any loss of optical power in the pulse stacking process can be compensated for by saturated amplification in the MPA. For a detailed description we refer the reader to Ref. [8].

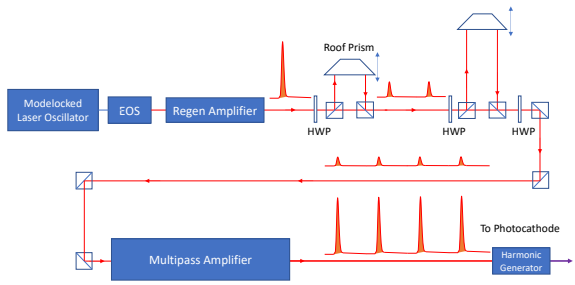

Figure 3: An example of IR split-and-delay setup for 4 bunches. A train of IR pulses is sent to the multi-pass amplifier (MPA) to recuperate the losses after splitting. It is then sent through the 3rd harmonic generator, in order to obtain high intensity UV pulse train.

BUNCH-BY-BUNCH TRAJECTORY CONTROL

The requirements for trajectory stability of the multi-bunch train are derived from the value for the single bunch. An example of single bunch position jitter in the HXR undulator is shown in Fig. 4. Typically at LCLS-HXR, trajectory jitter does not exceed 5-6 micron RMS.

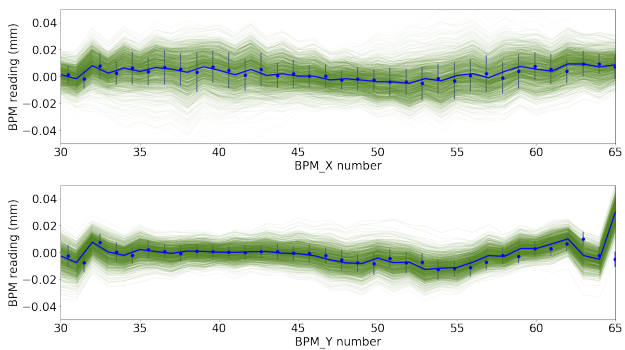

Figure 4: Single bunch HXR undulator orbit jitter at 10 GeV beam energy.

Currently, the LCLS multi-bunch performance is significantly impacted by the transverse RF kicks in the linac and differences in the RF amplitudes/phases for different bunches. The additional transverse RF kick comes from a slight pitch error of the RF cavities ϕ and can be calculated using $\Delta\theta \approx \phi\Delta P/P$. Here P is the relativistic momentum and ΔP is the momentum gain. A recent study of RF kicks in the LCLS linac is summarized in [9].

In order to provide bunch-by-bunch trajectory control in the undulators, we will use 4 ultra-fast classical stripline kickers, similar to what is discussed in [10]. A model of the stripline we are developing is presented in Fig. 5. We will power the striplines with a choice of two high-voltage sources. First source is based on ultra-fast dual step-recovery diode (DSRD) pulser, which can provide up to 10 kV at the electrodes. This option can be used as an additional kicker

ISBN: 978-3-95450-214-1 ISSN: 2673-5490 doi:10.18429/JACoW-IPAC2021-MOPAB098

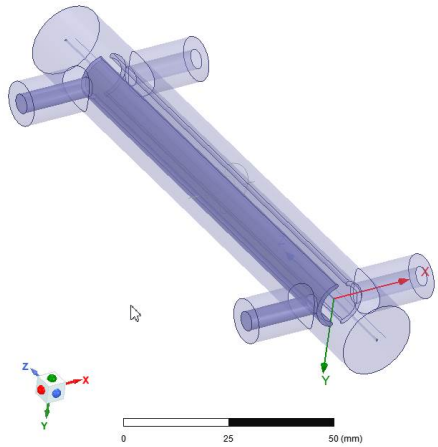

Figure 5: CAD model of the TEM stripline.

on day to day basis, or control the trajectories in two-bunch mode. The second power source is a broadband (10 kHz - 225 MHz) high power RF amplifier. Using the second option allows for bunch-by-bunch correction of arbitrary spaced trains. The stripline kickers will provide a beam angular kick θ defined by the relations:

$$\theta = \frac{2\int E_{\perp} dt}{E_{beam}/e} = \frac{\alpha}{E_{beam}[eV]}, \quad (1)$$

$$\alpha = \frac{2VL}{r}\frac{4}{\pi}\sin\frac{\psi}{2}, \quad (2)$$

where V is the applied voltage, L is the structure length, and ψ is the opening angle. One can then determine the corresponding orbital displacements as $\Delta x = \theta\beta_{x,y}$, where $\beta_{x,y}$ are the beta functions. The resulting orbit displacements as a function of RF amplifier power are presented in Fig. 6.

We analyze the striplines placement with a lattice response matrix [11–13]. The model response matrix $\mathrm{rMat}_{i,j} = da_i/d\theta_{a,j}$, where $a = X, Y$ is shown in Fig. 7. Given the linac real estate constraints, we selected two locations for (x, x', y, y') trajectory correction. These locations are depicted as white dashed lines in Fig. 7. The modelled phase advance between the structures is 72° in X- and 54° in Y-direction. In the real machine, the response matrix will be reconstructed from measurements, and the required kicks will be applied to individual bunches. In cases when electron bunches can not be resolved transversely, the XFEL tuning will be done by scanning the stripline amplitudes manually or via automated search.

SUMMARY

We presented a comprehensive plan towards more robust multi-bunch operation of the LCLS. When enabled, multi-bunch mode will allow for many new in-house and user experiments. It will also serve as test bed for future ultra-high repetition rate XFELs.

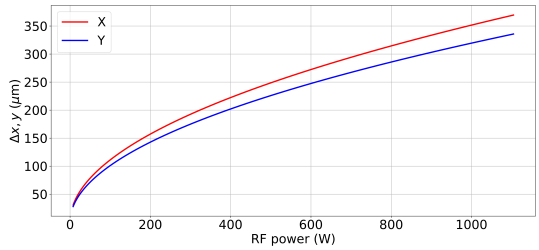

Figure 6: Trajectory displacement as a function of amplifier RF power at the stripline at linac 21-9 location.

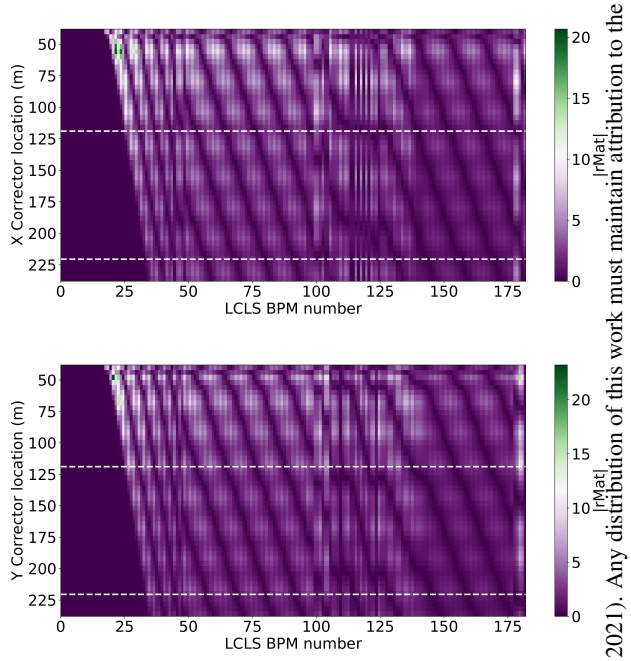

Figure 7: Modulus of the response X (top) and Y (bottom) matrices as a function of 50 corrector locations, equally spaced (Δz = 5 m) in the machine starting from BC1 location. Two dashed white lines correspond to 21-9 and 22-9 locations chosen for TEM stripline installation.

ACKNOWLEDGEMENTS

We would like to thank C. Pellegrini, Y. Ding, Z. Huang, G. Marcus, E. Galtier and S. Glenzer (SLAC), P. Piot (ANL/NIU), S. De Santis (LBL) for many valuable suggestions, M. Chahbazian (Amplifier Research) and R. Kobana (R&K) for technical consultations on amplifier performance. This work is supported by the U.S. Department of Energy Contract No. DE-AC02-76SF00515.

REFERENCES

[1] F.-J. Decker *et al.*, "A demonstration of multi-bunch operation in the LCLS", in *Proc. 32nd Int. Free Electron Laser Conf. (FEL'10)*, Malmö, Sweden, Aug. 2010, paper WEPB33, pp. 467–470.

[2] F.-J. Decker *et al.*, "Two bunches with ns-separation with LCLS", in *Proc. 37th Int. Free Electron Laser Conf.*

ISBN: 978-3-95450-214-1 ISSN: 2673-5490 doi:10.18429/JACoW-IPAC2021-MOPAB098

(FEL'15), Daejeon, Korea, Aug. 2015, pp. 634–638. doi:10.18429/JACoW-FEL2015-WEP023

[3] F.-J. Decker, K. L. F. Bane, W. S. Colocho, A. A. Lutman, and J. C. Sheppard, "Recent developments and plans for two bunch operation with up to 1 μs separation at LCLS", in *Proc. 38th Int. Free Electron Laser Conf. (FEL'17)*, Santa Fe, NM, USA, Aug. 2017, pp. 288–291. doi:10.18429/JACoW-FEL2017-TUP023

[4] F.-J. Decker *et al.*, "Four X-ray pulses within 10 ns at LCLS", in *Proc. 10th Int. Particle Accelerator Conf. (IPAC'19)*, Melbourne, Australia, May 2019, pp. 1859–1862. doi:10.18429/JACoW-IPAC2019-TUPRB086

[5] K.-J. Kim, Y. Shvyd'ko, and S. Reiche, "A proposal for an X-ray free-electron laser oscillator with an energy-recovery Linac", *Phys. Rev. Lett.*, vol. 100, p. 244 802, Jun. 2008. doi:10.1103/PhysRevLett.100.244802

[6] G. Marcus *et al.*, "Refractive guide switching a regenerative amplifier free-electron laser for high peak and average power hard X-rays", *Phys. Rev. Lett.*, vol. 125, p. 254 801, Dec. 2020. doi:10.1103/PhysRevLett.125.254801

[7] A. Halavanau *et al.*, "Population inversion X-ray laser oscillator", *Proc. Nat. Acad. Sci.*, vol. 117, no. 27, pp. 15 511–15 516, 2020. doi:10.1073/pnas.2005360117

[8] A. Halavanau *et al.*, "Double bunch FEL at LCLS-II", SLAC, Menlo Park, CA, USA, Tech. Rep. LCLS-II-TN-20-09, 2021.

[9] R. A. Margraf, F.-J. Decker, G. Marcus, and Z. Huang, "Measurement and correction of RF kicks in the LCLS accelerator to improve two-bunch operation", presented at the 12th Int. Particle Accelerator Conf. (IPAC'21), Campinas, Brazil, May 2021, paper TUPAB110, this conference.

[10] D. A. Goldberg and G. R. Lambertson, "Dynamic devices. A primer on pickups and kickers", *AIP Conf. Proc.*, vol. 249, no. 1, pp. 537–600, 1992. doi:10.1063/1.41979

[11] Y. C. Chao, "Orbit correction methods: Basic formulation, current application at Jefferson Lab, and future possibilities", CERN, Geneva, Switzerland, Tech. Rep. CERN-OPEN-2000-220, 1998.

[12] D. Sagan, "Bmad: A relativistic charged particle simulation library", *Nucl. Instrum. Meth. A*, vol. 558, pp. 356–359, 2006. doi:10.1016/j.nima.2005.11.001

[13] D. Sagan, The TAO manual, https://www.classe.cornell.edu/bmad/tao.html.